



Application of Discrete Element Parallel Bond Model in Rod Structures

Haitao Wang, Kun Zhou

School of Civil Engineering, Lanzhou University of Technology, Gansu, China

Corresponding author's e-mail address: zhoukun99@qq.com

First author's e-mail: 1791668665@qq.com

Abstract. In order to overcome the limitations of finite element in solving the rod structure, it is proposed to apply the particle discrete element method to study the force characteristics of the rod structure. This paper firstly introduces the advantages of discrete element relative to finite element, then describes the basic theory and calculation method of discrete element, finally, through the mutual comparison of the theoretical solution of cantilever steel beam, finite element solution and the discrete element solution by applying the parallel bond model, it is confirmed that the parallel bond model conforms to the intrinsic properties of the rod structure, and the parameter setting of the parallel bond model meets the requirement of the accuracy of the discrete element of rod system, and a set of parameters of the parallel bond model conforms to the intrinsic properties of Q235 steel.

Keywords: Discrete element method; Rod Structures; Parallel bond model

1 Introduction

The traditional Finite Element Method (FEM) used to simulate rod structures' mechanical behavior involves issues such as mesh distortion, element disappearance, displacement discontinuity, and stiffness matrix singularities [1]. To address these limitations, Cundall [2] introduced the Discrete Element Method (DEM), originally developed for discontinuous media but also applicable to continuous media problems [3]. Unlike FEM, DEM allows for relative motion between elements and does not necessarily require displacement continuity or deformation compatibility conditions. This feature makes it especially suitable for simulating large displacements, rotations, displacement discontinuities, and fracture material discontinuities in rod systems.

2 Basic Principle of Discrete Element Method

The principal idea of the discrete element method is to discretize the object of study into several rigid particles, which are connected by springs and dampers, as depicted in

© The Author(s) 2024

A. S. B. A Rashid et al. (eds.), *Proceedings of the 2024 3rd International Conference on Applied Mechanics and Engineering Structures (AMES 2024)*, Advances in Engineering Research 34,

https://doi.org/10.2991/978-94-6463-473-0_20

Fig. 1. The contact forces between particles are determined by the force-displacement criterion, and the motion of the particles is governed by the equation of motion (Newton's second law) [4]. The computational process of the discrete element method is illustrated in Fig. 2.



Fig. 1. Discrete element model of the beam element bar

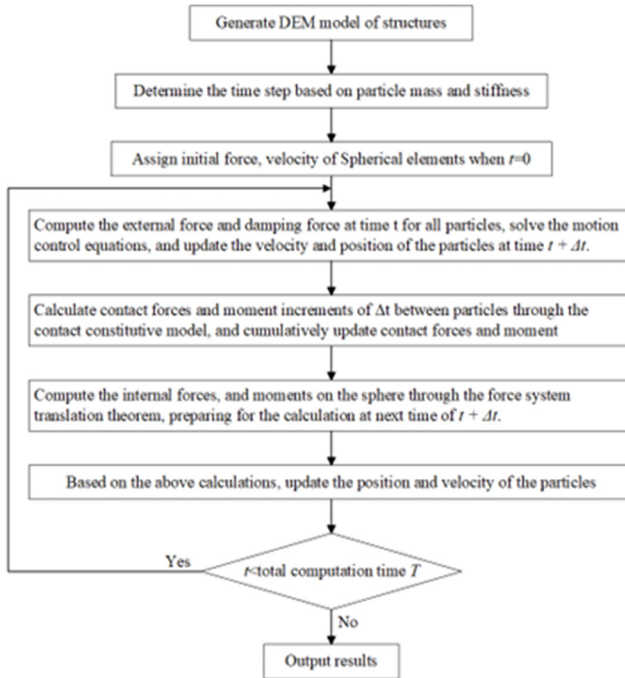


Fig. 2. Flow chart of discrete element method

2.1 Motion Control Equation

For spatial structures, the motion variables of the element can be decomposed into three translational displacements and three rotational displacements along the coordinate axes. Similarly, the mechanical state of the element can be de-composed into three forces and three moments of force along the coordinate axes.

Take any element a and its motion control equation can be expressed as follows:

$$\begin{pmatrix} m_a & & \\ & m_a & \\ & & m_a \end{pmatrix} \begin{pmatrix} \ddot{u}_x \\ \ddot{u}_y \\ \ddot{u}_z \end{pmatrix} = \begin{pmatrix} F_{x,int} \\ F_{y,int} \\ F_{z,int} \end{pmatrix} + \begin{pmatrix} F_{x,ext} \\ F_{y,ext} \\ F_{z,ext} \end{pmatrix} \quad (1)$$

$$\begin{pmatrix} I_{xx} & I_{xy} & I_{xz} \\ I_{yx} & I_{yy} & I_{yz} \\ I_{zx} & I_{zy} & I_{zz} \end{pmatrix} \begin{pmatrix} \ddot{\theta}_x \\ \ddot{\theta}_y \\ \ddot{\theta}_z \end{pmatrix} = \begin{pmatrix} M_{x,int} \\ M_{y,int} \\ M_{z,int} \end{pmatrix} + \begin{pmatrix} M_{x,ext} \\ M_{y,ext} \\ M_{z,ext} \end{pmatrix} = \begin{pmatrix} M_x \\ M_y \\ M_z \end{pmatrix} \quad (2)$$

where m_a is the mass of particle a, I_{ij} is the mass moment of inertia of particle a against the coordinate axes i and j, u_i is the horizontal displacement of particle a along the coordinate axis i, θ_i is the angular displacement of particle a around the coordinate axis i, $F_{i,int}$ and $F_{i,ext}$ are the combined internal force and combined external force on particle a along the coordinate axis i, respectively, and $M_{i,int}$, $M_{i,ext}$ and M_i are the combined internal moment, combined external moment, and total combined moment on particle a around the coordinate axis i, respectively.

2.2 Calculation Method of Solution

The basic solution methods for the discrete element include the dynamic relaxation method and the static relaxation method. The dynamic relaxation method is an explicit solution method, while the static relaxation method is an implicit solution method. The dynamic relaxation method is more widely used and is a numerical solution method that transforms nonlinear static problems into dynamic problems. It adopts a backward time-step iterative calculation idea, which introduces mass damping and stiffness damping that are less than critical damping, absorbs and dissipates the kinetic energy in the system, reduces the amplitude of vibration, and eliminates vibration. As a result, the system structure converges towards quasi-static values [5].

The dynamic relaxation method solves the displacements of the elements using the central difference method based on Newton's Second Law. The calculation begins from the known initial state. In one time step calculation process, all elements in the structure are first fixed. According to the contact constitutive relationship between the elements (force-displacement law), the contact internal forces and moments of the elements are determined and summed up with the external forces and moments acting on the elements to get the force state of the elements at the current time step. The central difference method is used to calculate the motion displacements of the relaxed elements. The elements are first relaxed, and then the relaxed elements are re-fixed in the new positions. Once the calculation of one element is completed, new contacts are formed with the adjacent elements, and the interaction forces between the elements change. The force state of the adjacent elements is updated and relaxation calculation is performed. This process is sequentially repeated for each element until all elements have been traversed. Once one time step calculation is completed, the calculation for the next time step begins [6].

The discrete element method employs an explicit integration method and the basic equation of motion of the discrete element method, taking into account the damping at the time t , can be expressed as follows:

$$\begin{cases} m\ddot{u}(t) = F_{\text{int}}(t) + F_{\text{ext}}(t) + F_{\text{damp}}(t) \\ I\ddot{\theta}(t) = M_{\text{int}}(t) + M_{\text{ext}}(t) + M_{\text{damp}}(t) \end{cases} \quad (3)$$

Where $\ddot{u}(t)$ and $\ddot{\theta}(t)$ are the translational linear acceleration and rotational angular acceleration, respectively, $F_{\text{int}}(t)$ and $M_{\text{int}}(t)$ are the particle contact combined internal force and combined internal moment, respectively, $F_{\text{ext}}(t)$ and $M_{\text{ext}}(t)$ are the particle contact combined external force and combined external moment, respectively.

$$\begin{cases} F_{\text{damp}}(t) = C_u \dot{u}(t) \\ M_{\text{damp}}(t) = C_\theta \dot{\theta}(t) \end{cases} \quad (4)$$

Where $F_{\text{damp}}(t)$ and $M_{\text{damp}}(t)$ are the damping of the element in the translation direction and the rotation direction, respectively, which can be either real or virtual damping. $\dot{u}(t)$, $\dot{\theta}(t)$ are the translation velocity and the rotation angular velocity, respectively, C_u and C_θ are the damping coefficients in the translation and rotation direction, respectively.

The explicit solution of the discrete element method adopts the central difference method and the first-order center difference for the velocity and acceleration of the elements is performed.

$$\begin{cases} \ddot{u}(t) = \left[\dot{u}\left(t + \frac{\Delta t}{2}\right) - \dot{u}\left(t - \frac{\Delta t}{2}\right) \right] / \Delta t \\ \dot{u}(t) = \left[\dot{u}\left(t + \frac{\Delta t}{2}\right) + \dot{u}\left(t - \frac{\Delta t}{2}\right) \right] / 2 \end{cases} \quad (5)$$

$$\begin{cases} \ddot{\theta}(t) = \left[\dot{\theta}\left(t + \frac{\Delta t}{2}\right) - \dot{\theta}\left(t - \frac{\Delta t}{2}\right) \right] / \Delta t \\ \dot{\theta}(t) = \left[\dot{\theta}\left(t + \frac{\Delta t}{2}\right) + \dot{\theta}\left(t - \frac{\Delta t}{2}\right) \right] / 2 \end{cases} \quad (6)$$

Substitute Eqs. (4), (5), and (6) into Eq. (3), and organize to obtain the iterative formula for the velocity at the adjacent time step. The velocity at time t is as follows:

$$\dot{u}\left(t + \frac{\Delta t}{2}\right) = \frac{2\Delta t(F_{\text{int}}(t) + F_{\text{ext}}(t)) + (2m + C_u\Delta t)\dot{u}\left(t - \frac{\Delta t}{2}\right)}{2m - C_u\Delta t} \quad (7)$$

$$\dot{\theta}\left(t + \frac{\Delta t}{2}\right) = \frac{2\Delta t(M_{\text{int}}(t) + M_{\text{ext}}(t)) + (2I + C_\theta\Delta t)\dot{\theta}\left(t - \frac{\Delta t}{2}\right)}{2I - C_\theta\Delta t} \quad (8)$$

From Eqs. (7) and (8), it can be observed that all the items on the right side of the equation are known, which simplifies the calculation process. The velocity at time can be directly obtained without the need for iteration, which improves computational efficiency. This demonstrates that the discrete element method does not need to solve large matrices or satisfy deformation compatibility conditions, making it suitable to deal with nonlinear large deformation problems.

3 Parallel Bond Model Theory and Parameter Validation

3.1 Parallel Bond Model Theory

The parallel bond model views the contact between particles as a collection of springs that are uniformly distributed on the contact surface. These springs have constant values for normal stiffness, tangential stiffness, and strength. And it is capable of transmitting both force and moment. The parallel bond contact model consists of two parts of interface mechanical behavior. The first interface behaves as a linear model that accommodates slip by applying a Coulomb limit to the shear force, without resisting relative rotation. The second interface, known as the parallel bond, acts in parallel with the first interface when bonded. When bonded, the second interface resists relative rotation and exhibits linear elastic behavior until the strength limit is surpassed, causing the bond to break and rendering it un-bonded. In the unbonded state, the second interface does not bear the load. The unbonded linear parallel bond model is essentially equivalent to the linear model [7].

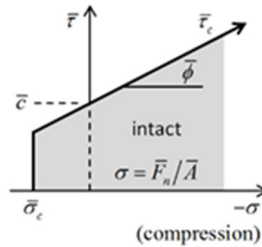


Fig. 3. Failure envelope for the parallel bond

In Fig. 3, when the parallel bond model is subjected to compression, the parallel bond contact will not be damaged. The parallel bond model always remains bonded while the compressive stress and shear stress continue to increase at the contact point. However, when the parallel bond model is subjected to tension, the contact shear stress decreases but the tensile stress increases up to (tensile stress limit). At this moment, the parallel bond breaks and the parallel bond model is equivalent to a linear contact model.

3.2 Validation of Parameter Settings for the Parallel Bond Model

In this section, the example employs Q235 steel and a cantilever beam with the beam length of 10 meters and the cross-sectional size of 500 mm × 500 mm. The theoretical

solution, finite element solution, and discrete element solution are compared and analyzed to validate the accuracy of the parameter settings for the parallel bond model.

(1) In the theoretical analysis of the cantilever beam, the relationship between the load applied at the free end of the beam and displacement at different positions along the axis of the beam can be represented as follows:

$$v = \frac{x^2 P(3L - x)}{6EI} \tag{9}$$

The relationship between the load at the free end of the cantilever beam and the stress at different positions of the axis of the beam is shown in the following equation:

$$\sigma = \frac{P(L - x)y}{I} \tag{10}$$

Where σ is the stress at the monitoring point of the cantilever beam, v is the displacement of the monitoring position of the cantilever beam, P is the load at the free end of the cantilever beam, x is the distance of the monitoring point from the fixed end, y is the distance from the stress monitoring point to the centroid axis of the cross-section, L is the length of the cantilever beam, E is the elastic modulus of the material, and I is the moment of inertia of the cross-section.

(2) Finite element numerical simulation analysis is conducted using the ANSYS Mechanical finite element module. As shown in Fig. 4, BEAM188 is selected for the beam element, BKIN is selected for the material model, the yield strength is 235MPa, the elastic modulus is $E=205\text{GPa}$, and the Poisson's ratio is 0.3.



Fig. 4. Diagram of the numerical finite element model

(3) Discrete element numerical simulation analysis is performed using the parallel bond contact model, as shown in Fig. 5. The particle spheres have a radius of 0.05 m. The spheres of the left end of the beam are fixed, while the center sphere of the free end of the beam applies a concentrate Load.



Fig. 5. Discrete element numerical model diagram

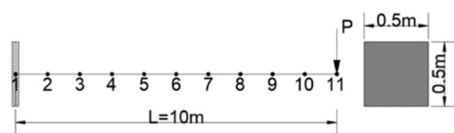


Fig. 6. Mechanical diagram of the cantilever beam and arrangement of monitoring points

Fig. 6 shows a schematic diagram of the mechanical calculation and the layout of 11 monitoring points for the cantilever beam. These monitoring points are set along the beam axis at intervals of 1 m to obtain stress and displacement data for these points.

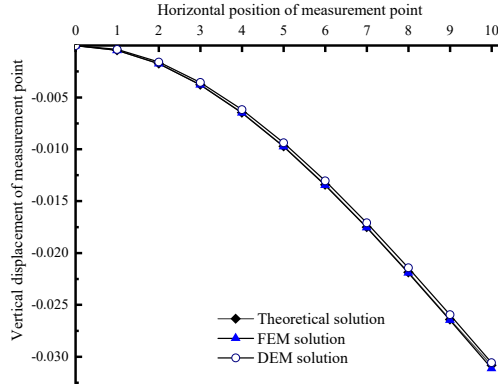


Fig. 7. Displacement curve of the cantilever beam

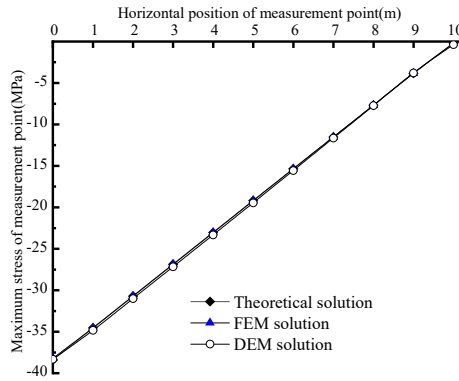


Fig. 8. The maximum stress curve of the cantilever beam monitoring point

Fig. 7 and Fig. 8 show the displacement and maximum stress curves at the monitoring points obtained via the theoretical method, finite element method, and discrete element method for the cantilever beam. From the figures, it can be observed that the numerical curves obtained from the three methods show similar trends, and the values of displacement and stress are close. The displacement errors of the finite element solution and the discrete element solution relative to the theoretical solution at the free end of the cantilever beam are 1% and 0.8%, respectively. The stress errors of both the finite element solution and the discrete element solution compared to the theoretical solution at the fixed end of the cantilever beam are within 1%. This indicates that the parameter settings of the parallel bond model are consistent with the constitutive relationship of Q235 steel. Additionally, the parallel bond model is suitable for the discrete element numerical simulation of structures made of Q235 steel.

4 Conclusions

This paper introduces the fundamental theory of the Discrete Element Method (DEM) and validates the correctness and rationality of applying the parallel bond constitutive model to rod structures through a comparative analysis of three numerical solutions for a cantilever steel beam. The main conclusions are as follows:

(1) This study confirms the parallel bond model's compliance with the solution accuracy of the Discrete Element Method (DEM) through three numerical solution methods for a cantilever beam, obtaining a set of parallel bond parameters for Q235 steel.

(2) The parallel bond model is consistent with the mechanical constitutive characteristics of rod structures.

(3) The rod system's Discrete Element Method, employing the parallel bond model, can serve as a novel approach for studying the mechanical behavior of rod structures under load.

Reference

1. Ye J, Xu L, Lu Z. Member Discrete Element Method for Static and Dynamic Responses Analysis of Steel Frames with Semi-Rigid Joints[J]. *Applied Sciences*, 2017, 7(7).
2. Cundall P A, Strack O D L. A discrete numerical model for granular assemblies[J]. *Geotechnique*, 1979, 29(1): 47-65.
3. Damien A, Angel M C. A DEM bonded particle model compatible with stress/strain constitutive relations [J]. *International Journal of Rock Mechanics and Mining Sciences*, 2023, 170.
4. Tuo W, Fengshou Z, Jason F, et al. A review of methods, applications and limitations for incorporating fluid flow in the discrete element method[J]. *Journal of Rock Mechanics and Geotechnical Engineering*, 2022, 14(3).
5. Jensen R P, Bosscher P J, Plesha M E, et al. DEM simulation of granular media—structure interface: effects of surface roughness and particle shape[J]. *International Journal for Numerical and Analytical Methods in Geomechanics*, 1999, 23(6).
6. Zhaowang Xia, Xiandong Liu, Yingchun Shan, Xinghu Li. Coupling Simulation Algorithm of Discrete Element Method and Finite Element Method for Particle Damper[J]. *Journal of Low Frequency Noise Vibration and Active Control*, 2009, 28(3):197-204.
7. Particle Flow Code in 3 Dimensionas. PFC3D version 5.0[R]. Minneapolis: Itasca Consulting Group Inc, 2014

Open Access This chapter is licensed under the terms of the Creative Commons Attribution-NonCommercial 4.0 International License (<http://creativecommons.org/licenses/by-nc/4.0/>), which permits any noncommercial use, sharing, adaptation, distribution and reproduction in any medium or format, as long as you give appropriate credit to the original author(s) and the source, provide a link to the Creative Commons license and indicate if changes were made.

The images or other third party material in this chapter are included in the chapter's Creative Commons license, unless indicated otherwise in a credit line to the material. If material is not included in the chapter's Creative Commons license and your intended use is not permitted by statutory regulation or exceeds the permitted use, you will need to obtain permission directly from the copyright holder.

